High-Performance Insulation Materials from Poly(ether imide)/Boron Nitride Nanosheets with Enhanced DC Breakdown Strength and Thermal Stability

He Li, Zongliang Xie, Lilan Liu and **Zongren Peng**
Xi'an Jiaotong University
State Key Laboratory of Electrical Insulation and Power Equipment, School of Electrical Engineering
Xi'an, Shaanxi 710049, China

Qisheng Ding, Lulu Ren, Ding Ai, Wuttichai Reainthippayasakul, Yuqi Huang and **Qing Wang**
The Pennsylvania State University
Department of Materials Science and Engineering
University Park, PA 16802, USA

ABSTRACT

Environmentally-friendly polymers which can be recycled and reused at the end of life are urgently needed for the development of advanced high-voltage direct current (HVDC) systems. Polymer nanocomposites have attracted considerable attention owing to their unique features arising from synergistic combination of inorganic fillers and polymer matrices. Here we describe thermoplastic poly(ether imide) (PEI) nanocomposites that contain boron nitride nanosheets (BNNSs). It is found that the polymer nanocomposites exhibit simultaneous improvements in multiple physical properties, such as the DC electrical breakdown strength, volume resistivity, mechanical strength and thermal stability, along with substantial reduction in loss tangent, compared with neat PEI. A great improvement in thermal conductivity has been attributed to the presence of BNNSs in the composites, which improves heat dissipation in comparison with neat polymers. The composite approach provides a promising solution for alleviating temperature-gradient distribution and addressing heat accumulation issues in HVDC equipment, and enables broader applications of insulation materials in HVDC systems operated under high voltages.

Index Terms — **polymer nanocomposites, HVDC insulation, electrical breakdown, thermal conductivity, thermal stability**

1 INTRODUCTION

POLYMERIC materials possess the intrinsic advantages of scalability, ease fabrication, mechanical flexibility, outstanding corrosion resistance, high electrical breakdown strength, high electric resistivity and low dielectric loss and are widely used as insulation materials in electronic devices and power equipment [1–3]. With ever-increasing demand and consumption of electric energy, advanced power system, especially high-voltage direct current (HVDC) transmission system, are increasingly important owing to its unique advantages in long-distance and large-capacity power transmission and grid interconnections [4, 5]. Accordingly, with HVDC transmission becoming the main trend of power grids, insulation materials for HVDC systems with high performance such as enhanced dielectric strength, mechanical strength, thermal conductivity and thermal stability are urgently needed.

Currently, epoxy resin and its composites were extensively used as main insulation materials in high-voltage dry-type bushing, gas-insulated switchgear (GIS) and gas-insulated metal enclosed transmission line (GIL) owing to their excellent processibility and good dielectric, mechanical and adhesion strength [2, 6]. In addition, cross-linked polyethylene (XLPE) has been used as an ideal insulation material for most extruded high-voltage cables. XLPE not only maintains the superb insulation properties of polyethylene (PE) but also improves the thermal stability and

Manuscript received on 28 June 2018, in final form 4 December 2018, accepted xx Month 20yy. Corresponding author: Q. Wang.

thermo-mechanical strength because of network structure via chemical cross-linking reaction [7]. However, it needs to be pointed out that both thermosetting materials and cross-linked thermoplastics are environmentally-unfriendly because they are difficult to be directly recycled and reused at the end of lifetimes. Nowadays, as minimizing the impact of human activities on the environment becomes an inevitable choice for sustainable development, "green" recyclable insulation materials has been intensively explored. In recent years, numerous studies focus on thermoplastic polymers, *e.g.*, low-density polyethylene (LDPE), high-density polyethylene (HDPE) and polypropylene (PP) [4, 8, 9], all of which exhibit outstanding insulation and corrosion-resistant properties. More recently, the polymer blends have been developed as HVDC insulation materials. He and coworkers [10] introduced polyolefin elastomer (POE) to increase the flexibility of PP. Du *et al* [11] investigated the effects of mechanical stretching on space charge behaviors of PP/POE blends. Huang *et al* [*1*2] evaluated the potential applications of isotactic PPs, propylene-ethylene block copolymers, propylene-ethylene binary random copolymers and propylene-ethylene-butene ternary random copolymers for HVDC cable insulations

However, the relatively low melting temperature of LDPE (i.e. ~ 112 ºC) limit their usage at elevated temperatures [4, 8]. Although PP displays a higher melting temperature of ~165 ºC along with a better long-term operating temperature of ~90 ºC in comparison to PE [4, 9], the mechanical and dielectric strengths of PP still decrease rapidly with increasing temperatures above 105 ºC [13]. More serious issues arise from the well-recognized poor thermal conductivities of polymeric materials (i.e. ~ 0.1–0.5 W/m/K) [14]. During the high-voltage operation, dielectric loss of insulation materials is converted into joule heat, giving rise to temperature gradients as well as resistivity gradients in power equipment such as power cables especially under high fields because of the poor thermal conductivities of polymeric materials [15]. Subsequently, this results in the reduction of insulation strength and the acceleration of aging processes, which severely restricts the development of HVDC system operating at higher voltages. Thus, novel insulation materials with high thermal stability and thermal conductivity is vitally needed for HVDC equipment.

Poly(ether imide) (PEI), a modified version of polyimide, is a class of recyclable thermoplastic amorphous polymers with excellent mechanical strength, insulation properties and chemical durability. PEI has a higher glass transition temperature (T_g) of about 217 ºC and greater thermal stability when compared to PE and PP [16]. In terms of electrical engineering applications, PEIs have been used as capacitor thin films in DC-DC converters and as insulating components in high-voltage switchgears [13, 17], but have not been fully exploited in HVDC equipment due to the relatively high production cost and high technical requirements on processing [17]. Although PEI shows its potential as a promising high-temperature polymer for HVDC equipment, the relatively higher loss tangent and lower electrical breakdown strength than non-polar polymers *e.g.* PP, along with its low thermal conductivity, need to be addressed [16].

In recent years, the introduction of high-thermal-conductivity inorganic components *e.g.* aluminum oxide (Al_2O_3), aluminum nitride (AlN) and boron nitride (BN), into polymer matrices to form polymer composites is an emerging and promising approach to electrical insulation materials with enhanced thermally conductive properties [3, 14, 16]. It is noteworthy that hexagonal boron nitride (*h*-BN), the most stable crystalline form of BN, which displays not only the advantages of the (002) face of a graphitic-like structure such as excellent thermal conductivity (~ 300 W/m/K) [18] but also low leakage currents and high breakdown strength (~ 800 MV/m) as a wide band-gap insulator [1, 19]. More interestingly, it is found that the breakdown field of *h*-BN can be further increased by decreasing the thickness of *h*-BN powders to boron nitride nanosheets (BNNSs) with few layers [20]. Numerous studies have focused on the polymer composites filled with BN, in which enhanced dielectric and thermal properties were obtained [1, 19, 21–23]. Wang and coworkers fabricated a class of BNNS-filled polymer nanocomposites using various polymer matrices *e.g.*, crosslinked divinyltetramethyldisiloxane-bis(benzocyclobutene) (*c*-BCB) [1], poly(vinylidene fluoride-triuoroethylene-chlorouoroethylene) (P(VDF-TrFE-CFE)) [19], and poly(methyl methacrylate) (PMMA) [21]. It is found that synergistic improvements in the dielectric and mechanical strength and thermal conductivity were achieved in the resulting nanocomposites. Du *et al* [22] mixed hybrid BN filler into LDPE matrix and a thermal conductivity of 0.95 W/m/K was obtained in the LDPE/BN composite with 40 wt% filler loading. In addition, Dang and coworkers [23] fabricated ternary BNNSs/SEBS/PP nanocomposites by melt-mixing of BNNSs and SEBS with PP matrix, the thermal conductivity of the nanocomposites increases to 0.95 W/m/K with a relatively low loading of BNNSs.

Herein, we describe the development of high-performance insulation materials via a composite approach based on PEI as a recyclable polymer matrix and ultra-thin two-dimensional BNNSs as the fillers for potential HVDC applications. The homogeneously-dispersed BNNSs in PEI not only improve the electrical breakdown strength and DC electric resistivity but also reduce dielectric loss. Additionally, multiple properties including thermal conductivity and Young's modulus are simultaneously enhanced in comparison to neat PEI. Notably, the PEI/BNNSs nanocomposites exhibit outstanding thermal stabilities (i.e. ≥150 ºC) and marked improvements in temperature-dependent electrical breakdown strength with respect to PE and PP.

2 EXPERIMENTAL

2.1 EXFOLIATION OF BNNS

BNNSs were prepared through liquid-phase exfoliation of *h*-BN powders [19, 21]. 4 g *h*-BN powders (Sigma-Aldrich) were dispersed in 300 ml dimethylformamide (DMF) (Sigma-Aldrich) under vigorous stirring. A tip-type sonication (175 W) was conducted to exfoliate BN for 48 hours. The resultant mixture was first centrifuged at 3000 rpm for 40 min, and the supernatant was collected and unexfoliated *h*-BN powders were removed. The collected supernatant was subjected to a centrifugation at 10000 rpm for 20 min to precipitate nanosheets. Exfoliated BNNSs was obtained after vacuum drying at 70 ºC for 12 h.

2.2 PREPARATION OF PEI/BNNS NANOCOMPOSITE FILMS

PEI (Poly*K* Technologies) pellets were dissolved in *N*-methyl pyrrolidone (NMP) (Sigma-Aldrich) and stirred overnight at 40 ºC to yield a clear and transparent solution. The BNNS dispersion with various concentrations was prepared in NMP by tip-type sonication (175 W) for 1 h, which was then mixed with PEI solution. The mixture was further sonicated for another 30 min, and then drop-casted on a re-cleaned glass plate. The cast films were dried at 120 ºC for 12 h, and subsequently peeled off from the substrates in deionized (DI) water followed by drying in a vacuum at 120 ºC for another 12 h to remove solvent residue and water. The typical thickness of nanocomposite films is 8–14 μm.

2.3 PREPARATION OF LDPE AND PP FILMS

LDPE (Sigma-Aldrich) pellets and isotactic PP (Sigma-Aldrich) pellets were pre-heated in a hydraulic press machine at 170 ºC and 220 ºC for 10 min, respectively. Both polymers were then hot-pressed by the increasing pressure of 500 psi every 5 minutes up to 2500 psi. The LDPE and PP films with an average thickness of 10–16 μm were obtained by naturally cooling at the holding pressure.

2.4 CHARACTERIZATION

The nanofiller structure was characterized using a FEI Talos F200X transmission electron microscopy (TEM) by placing a few drops of dispersion on a lacey carbon covered copper grid, and evaporating it prior to observation. The cross-sectional morphologies were taken using a FEI NanoSEM 630 field emission scanning electron microscope (SEM). Fourier transform infrared (FTIR) spectra were conducted on a Varian Digilab FTS-8010 spectrometer at room temperature. FTIR of polymeric films were collected in the attenuated total reflectance (ATR) mode using ZnSe crystal as a contact to the samples, and nanofiller were mixed with potassium bromide (KBr) using a transmission mode. X-ray diffraction (XRD) measurement was conducted by a PANalytical X'pert Pro MPD theta–theta diffractometer. Gold electrodes of a diameter of 3 mm and a thickness of 60 nm were sputtered on both sides of the films for all the electrical measurements. Dielectric spectra were acquired over a broad frequency range (10^2–10^6 Hz) using a Hewlett Packard 4284A LCR meter. Direct-current (DC) steady state conductance currents were obtained under a relatively high electric field (100 MV/m) provided by a Hewlett Packard 4140B pA meter/voltage source and TREK model 2210 amplifier in a Delta Design oven model 2300 equipped with a liquid nitrogen cooling system. Electrical breakdown strength measurements were performed on a TREK P0621P instrument using the electrostatic pull-down method under a DC voltage ramp of 500 V/s. Measurements were performed in Galden HT insulation fluid using a digital hot plate equipped with a thermal couple to control the temperature. Young's moduli were derived from strain–stress curves measured with a TA RSA-G2 Solid Analyzer using a constant linear stretching rate of 0.02%/s. Thermal conductivity measurements were based upon a transient technique using a Hot Disk AB thermal analyzer with a sensor of type 7854 (20.96 mm diameter) being placed between two thin samples The sensor supplied a heat-pulse of 1 W for 20 s to the sample and the associated change in temperature was recorded. Thermogravimetric analysis (TGA) measurements were performed with a TA Q600 instrument at a heating rate of 20 ºC/min under nitrogen atmosphere.

3 RESULTS AND ANALYSIS

3.1 STRUCTURAL CHARACTERIZATIONS

The chemical structure of PEI can be seen in Figure 1. The presence of flexible ether linkages incorporated into the backbone of PEI through the nucleophilic aromatic substitution of leaving groups from phthalic anhydride by bisphenol A brings the solvability in polar solvents like NMP, providing the possibility for homogeneous dispersion of BNNSs in polymer matrix [16].

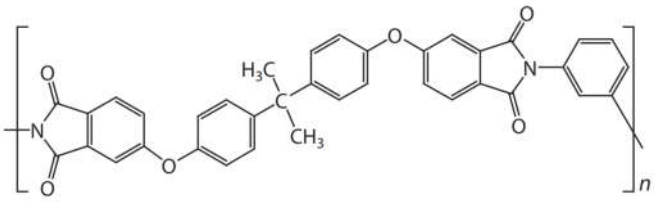

Figure 1. Chemical Structure of PEI.

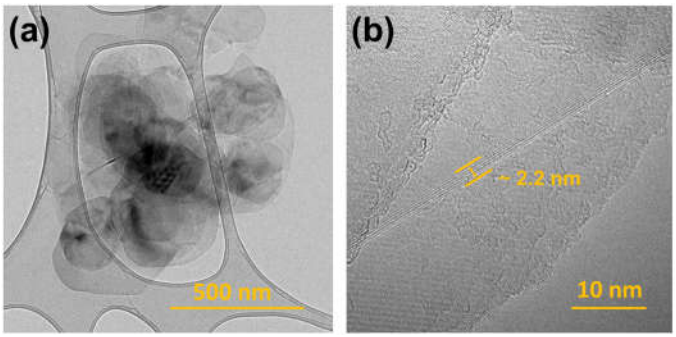

Figure 2. (a) Low-resolution TEM image of BNNSs. (b) High-resolution TEM image of BNNSs with exposed edge showing the layer feature.

Our previous work [19] has demonstrated that the majority of BNNSs exfoliated via the solution-sonication method is around 2 nm (i.e. 2~6-layer sheets) in thickness and 400 nm in lateral size, which is confirmed by low- and high-resolution TEM images shown in Figure 2. Figure 3a is the cross-sectional SEM image of neat PEI. Figure 3b shows stable suspensions of ultra-thin BNNSs in NMP. Accordingly, as seen in Figure 3c, dense network-like structures are formed in the solution-casted PEI/BNNSs nanocomposite, which confirms homogeneous filler dispersion even at 10 wt% of the filler loading in PEI.

The FTIR spectra of BNNS, neat PEI and the PEI nanocomposite with 10 wt% BNNSs are shown in Figure 4. The presence of BNNS is confirmed by the emergence of the characteristic peaks centered at 813 cm^{-1} and 1375 cm^{-1} in the spectrum of PEI/BNNSs, which are assigned to the out-of-plane and in-plane ring vibration of *h*-BN, respectively [1, 22].

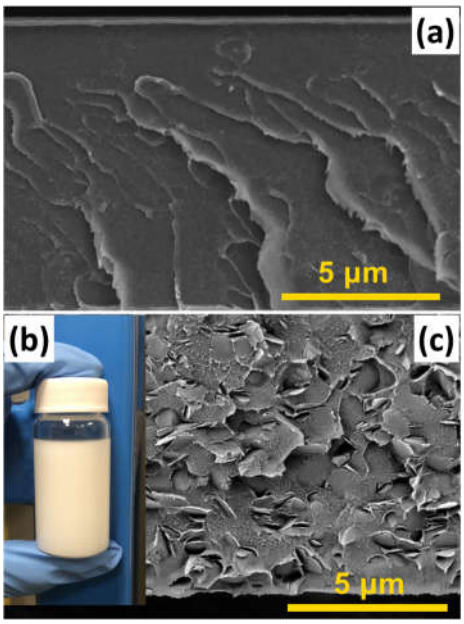

Figure 3. (a) Cross-sectional SEM image of neat PEI. (b) BNNSs dissolved in NMP at a concentration of 4 mg/mL. (c) Cross-sectional SEM image of the PEI nanocomposite with 10 wt% BNNSs.

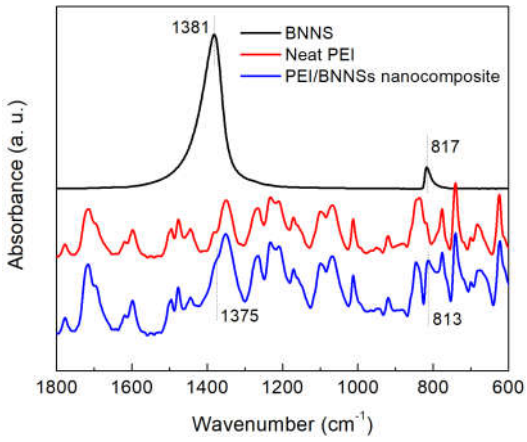

Figure 4. FTIR spectra of BNNS, neat PEI and the PEI nanocomposite with 10 wt% BNNSs.

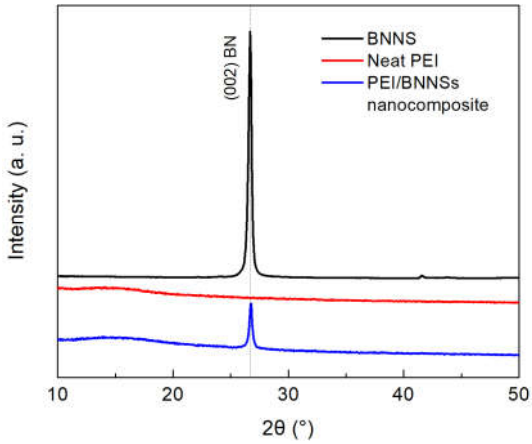

Figure 5. XRD patterns of BNNS, neat PEI and the PEI nanocomposite with 10 wt% BNNSs.

XRD patterns of BNNS, neat PEI and the PEI nanocomposite with 10 wt% BNNSs are presented in Figure 5. It is found that the introduction of BNNSs into PEI does not change the amorphous nature of PEI. The shape characteristic peak at $2\theta = 26.7^{o}$ refers to the hexagonal symmetry of (002) BN [1, 20].

3.2 WEAK-FIELD DIELECTRIC PROPERTIES

Real part of permittivity (K) and loss tangent ($\tan\delta$) of neat PEI and the PEI/BNNSs nanocomposites measured at room temperature are shown in Figure 6. The K value of the PEI nanocomposites increases moderately with the increase of BNNS loading, *e.g.*, from 3.26 of neat PEI to 3.44 of the PEI nanocomposite with 14 wt% BNNSs measured at 10^3 Hz. The modest improvement in K is because of the relatively higher K (~ 4) of BNNS filler compared with PEI and the enhanced interfacial polarization between nanofiller and polymer matrix [19]. Notably, the $\tan\delta$ is sharply decreases from neat PEI to the nanocomposites, *e.g.*, at 10^3 Hz, from 0.0084 of neat PEI to 0.0053 of the nanocomposite with 12 wt% BNNSs, which is apparently owing to low loss of wide band-gap (~ 6 eV) BNNS fillers [1, 24].

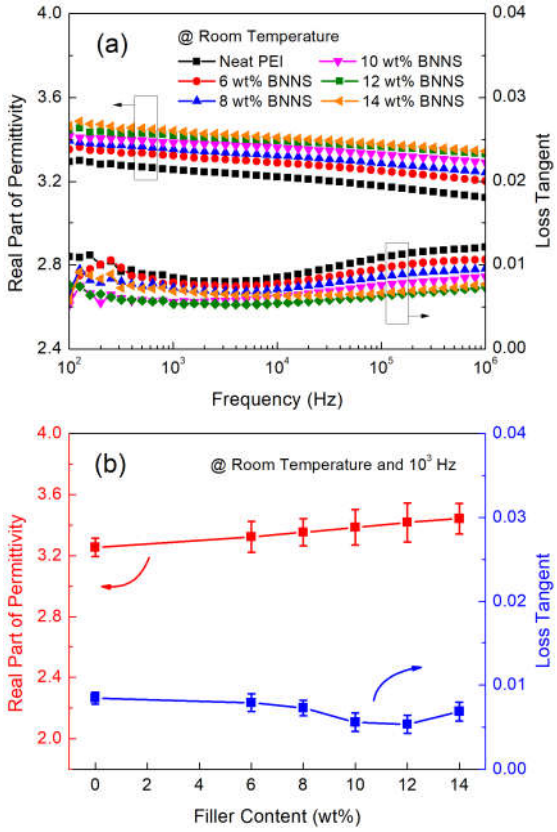

Figure 6. (a) Frequency-dependent dielectric properties of neat PEI and the PEI nanocomposites with varied BNNS contents. (b) Dielectric properties of the PEI nanocomposites at 10^3 Hz as a function of BNNS content.

3.3 DC ELECTRICAL BREAKDOWN STRENGTH

DC electrical breakdown strength of neat PEI and the PEI/BNNSs nanocomposites has been analyzed based on a two-parameter Weibull distribution function given by:

$$P(E) = 1 - \exp(-(\frac{E}{\alpha})^{\beta}) \quad (1)$$

where $P(E)$ is the probability of breakdown strength at a certain electric field, E is the measured breakdown field. Scale parameter α is the field strength for which there is a 63.2 %

probability of breakdown (Weibull breakdown strength) and shape parameter β evaluates the scatter of experimental data. Figure 7 shows the Weibull plot of the electric breakdown data of neat PEI and the PEI nanocomposites with various BNNS loadings measured at room temperature and 150 ºC, respectively. The 95 % confidence interval (±), the Weibull parameters α and β were calculated and listed in Table 1.

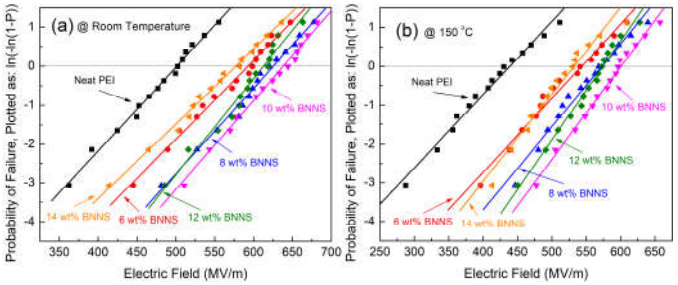

Figure 7. Weibull plots of neat PEI and the PEI nanocomposites with various BNNS loadings measured at (a) room temperature and (b) 150 ºC.

Table 1. 95% Confidence interval (±) of breakdown strength data and the scale parameter α and shape parameter β from the Weibull statistics.

	Room temperature			150 ºC		
	±	α (MV/m)	β	±	α (MV/m)	β
PEI	208.75	501	10.79	237.87	439	7.46
6 wt%	222.23	593	11.97	234.36	543	9.6
8 wt%	203.3	625	13.79	208.69	573	11.6
10 wt%	195.41	638	14.64	188.17	599	13.45
12 wt%	179.84	613	15.17	175.86	575	13.59
14 wt%	233.73	577	11.1	197.66	532	11.38

As summarized in Table 1, at room temperature, the Weibull breakdown strength of the PEI nanocomposites reaches to the highest value of 638 MV/m at 10 wt% BNNS, which corresponds to almost 30 % improvement with respect to that of neat PEI (i.e. 501 MV/m). Simultaneously, a marked enhancement of β is found in the PEI/BNNSs nanocomposites, *e.g.*, from 10.79 of neat PEI to 15.17 of 12 wt% PEI/BNNSs nanocomposite, standing for improved dielectric reliability of the resulting materials. In terms of temperature-dependent breakdown, although both neat polymer and the composites show steady decrease of Weibull breakdown strength with the increase of temperature from room temperature to 150 ºC, the reduction in Weibull breakdown strength of the composites is much less than that of neat polymer. For example, the α values decrease by 12.4 % for neat PEI but 6.1 % for the PEI nanocomposite with 10 wt% BNNS; this suggests that greatly enhanced thermo-dielectric stability is obtained in two-dimensional BNNS filled nanocomposites.

3.4 DC VOLUME RESISTIVITY

DC volume resistivity of neat PEI and the PEI/BNNSs nanocomposites calculated from steady state conductance current is shown in Figure 8. Compared with neat PEI, substantial enhancement in DC volume resistivity is found in the PEI/BNNSs nanocomposites. For example, at room temperature, a resistivity value of 6.4×10^{15} Ω m is determined in the PEI nanocomposite with 12 wt% BNNSs, which is about half order of magnitude higher than that of PEI (i.e. 1.22×10^{15} Ω m). Interestingly, the PEI/BNNSs nanocomposites exhibit greater temperature-dependent stability of insulation properties in comparison with neat PEI, *e.g.*, the resistivity of neat PEI decreases to 3.05×10^{12} Ω m with the temperature increases to 150 ºC, whereas the corresponding resistivity is 1.94×10^{13} Ω m for 12 wt% PEI/BNNSs nanocomposite.

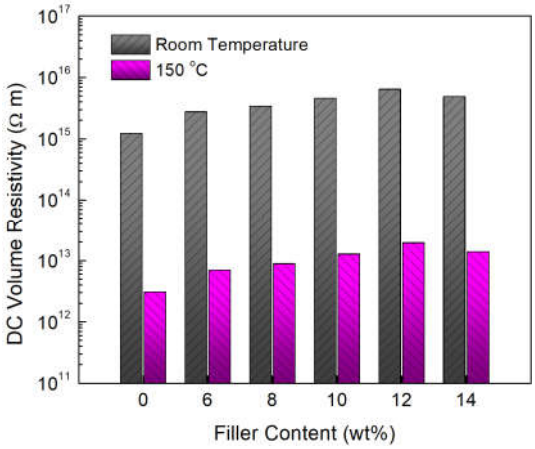

Figure 8. DC volume resistivity of the PEI nanocomposites at room temperature and 150 ºC as a function of BNNS content.

3.5 YOUNG'S MODULUS

The Young's modulus, which can be used to evaluate the electromechanical failure caused by mutual coulombic force from the opposite electrodes under an applied electric field [25], are analyzed for neat PEI and the PEI nanocomposite with 10 wt% BNNSs at varied temperatures. As seen in Figure 9, higher moduli of the composites are direct results of the introduced BNNSs in comparison with neat PEI, *e.g.*, from 0.77 GPa of neat PEI to almost 1 GPa of 10 wt% PEI/BNNSs nanocomposite measured at room temperature. In addition to the improved temperature-dependent dielectric strength, the nanocomposite also exhibits greater thermo-mechanical stability. For example, the Young's modulus decreases by more than 60% for neat PEI from room temperature to 150 ºC in comparison to less than 40% reduction for the PEI/BNNSs nanocomposites.

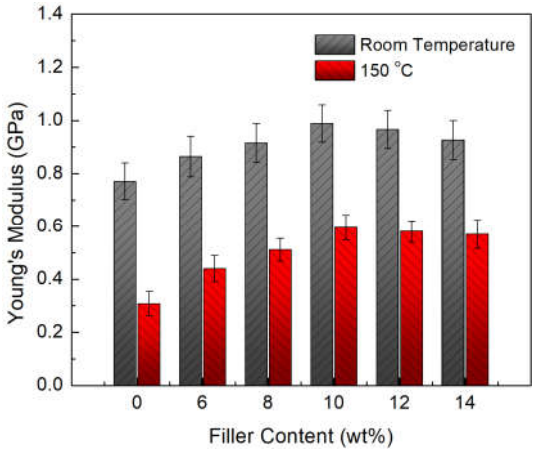

Figure 9. Young's modulus of the PEI nanocomposites at room temperature and 150 ºC as a function of BNNS content.

3.6 THERMAL CONDUCTIVITY

The thermal conductivity of polymeric materials is well-known orders of magnitude lower than those of ceramic and

metallic materials [14]. As can be seen in Figure 10, the thermal conductivity is improved by nearly 5 times from 0.22 W/m/K of neat PEI to almost 1 W/m/K of the nanocomposite with 14 wt% BNNSs. The enhancement of thermal conductivity in the nanocomposites is attributed to the much higher value of thermal conductivity of BNNS filler compared with host polymer and the formation of the interconnected thermal conductive structures by two-dimensional BNNS fillers with large specific surface area and high aspect ratio [1, 19].

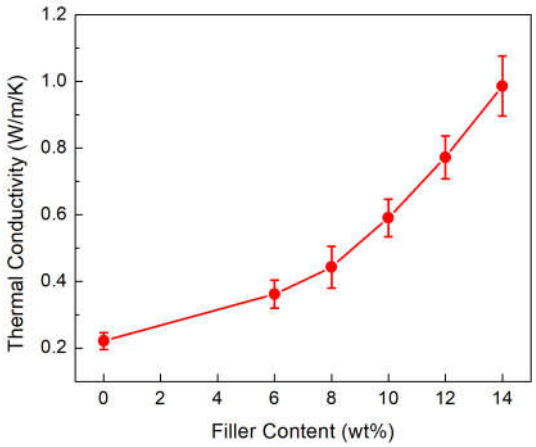

Figure 10. Thermal conductivity of the PEI nanocomposites as a function of BNNS content.

3.7 THERMOGRAVIMETRIC ANALYSIS

TGA curves of neat PEI and the PEI nanocomposite with 10 wt% BNNSs are shown in Figure 11. The thermal decomposition temperature with 5% weight loss is marked as $T_{95\%}$. $T_{95\%}$ of PEI is around 547 °C, proving the excellent thermal stability of the polymer. Notably, $T_{95\%}$ shifts to a higher temperature, i.e. 551 °C, upon the introduction of BNNSs into PEI, suggesting that the thermal stability of the host polymer is further enhanced by the inorganic nanofillers.

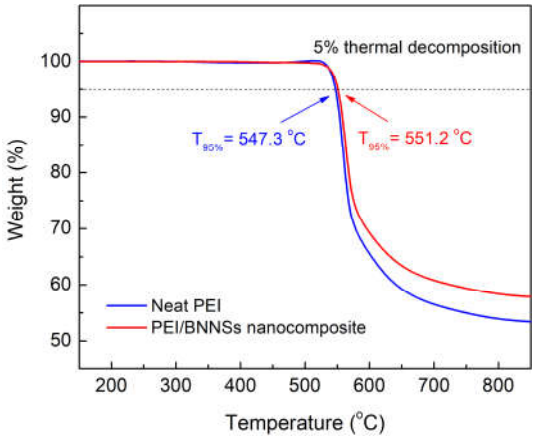

Figure 11. TGA curves of neat PEI and the PEI nanocomposite with 10 wt% BNNSs.

4 DISCUSSION

In an effort to understand the greatly synergetic enhancement of dielectric strength, mechanical strength and thermal conductivity as well as the largely reduced dielectric loss in the resultant PEI/BNNSs nanocomposites, the effects of the introduced BNNSs are systematically evaluated.

Since the polar surface of BNNS induced by the B–N bonds provide a good compatibility between the inorganic and polar organic phases, the PEI nanocomposites with homogeneous filler dispersion are obtained *via* a simple solution-casting method without any further surface functionalization. Different from melt-extrusion, solution processing enables homogeneous dispersion of fillers in the polymer matrix. In terms of dielectric loss, the incorporation of BNNS into the polymer not only contributes to a notable reduction in weak-field loss but also effectively decreases the DC conduction loss under high electric fields. It is found that interconnected insulation networks are formed by two-dimensional ultra-thin BNNSs with wide band-gap, which functions as charge-blocking barrier and reduces the high-field dielectric losses. The loss tangent decreases and the electrical resistivity of the composites increases with increasing the BNNS content up to 12 wt%. The further increase of the BNNS content beyond 12 wt% leads to the increase of the loss tangent and the reduction in the electrical resistivity of the composites. This is apparently due to the formation of agglomerates and defects, *e.g.*, voids and micro-cracks, at the polymer–inorganic filler interfaces. As evidenced in the cross-sectional SEM images of the PEI nanocomposites with high filler loadings. Consequently, the formation of agglomerates and defects decreases the breakdown strength of the composites [2, 3]. In general, the breakdown strength of dielectric materials is generally governed by a number of mechanisms. Polymers with reduced loss tangent and low DC conductance current usually exhibit high electrical breakdown strength [2]. Besides, higher Young's modulus of the composites arising from the introduced BNNS create a robust scaffold, which could provide better capacity to withstand the coulombic force caused from the opposite electrodes under an applied electric field, *i.e.*, impeding the occurrence of electromechanical failure [16, 25]. Although the calculated electromechanical breakdown strengths show the same trend as the experimental Weibull breakdown data, the calculated values are more than an order of magnitude higher than the experimental data. This is consistent with the earlier results on the dielectric composites [19]. The electromechanical breakdown model is known to work best for soft polymer dielectrics such as polyethylene, especially at the temperature that is above the glass transition temperature (T_g) or melting temperature (T_m) of the polymer [16]. The temperature range in our study is from room temperature to 150 °C, which is much below the T_g of PEI matrix (i.e. 217 °C). Therefore, the electromechanical breakdown strength which is mainly determined by the Young's modulus can not be solely account for the electrical breakdown of the PEI/BNNSs composites.

In addition, the thermal stability of PEI and the PEI/BNNSs nanocomposites is characterized in comparison with that of LDPE and PP, which are commercial polymers for HVDC equipment. Figure 12 shows the temperature-dependent Weibull breakdown strength of LDPE, PP, PEI and the PEI nanocomposite with 10 wt% BNNSs. Large reductions of the breakdown strength are found in neat polymers, which are 37.4%

for LDPE from room temperature to 80 ºC, 13.5% for PP from room temperature to 105 ºC, and 12.4% for PEI from room temperature to 150 ºC. On the other hand, the nanocomposite exhibits relatively stable thermo-dielectric performance with only 6% decrease from room temperature to 150 ºC. Similarly, both electrical resistivity and Young's modulus of the nanocomposites exhibit greater thermal stability in comparison with neat PEI. These results could be attributed to the presence of BNNS, which improves the thermal conductivity via the formation of the heat dissipation channels constructed by BNNSs.

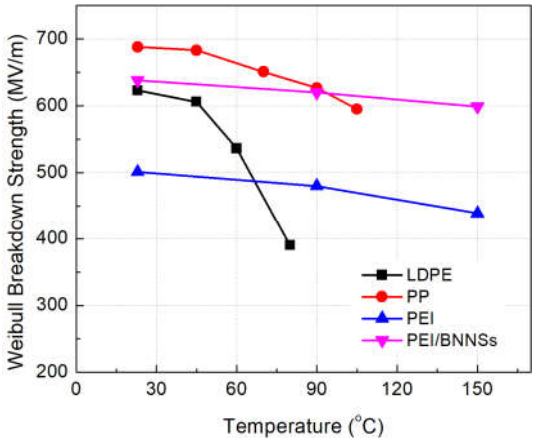

Figure 12. Temperature-dependent Weibull breakdown strength of LDPE, PP, PEI and the PEI nanocomposite with 10 wt% BNNSs.

5 CONCLUSIONS

In this work, the well-dispersed nanocomposites filled with ultra-thin BNNSs based on recyclable PEI matrix have been prepared by facilely solution processing. The resultant composites exhibit greatly enhanced DC breakdown strength, DC volume resistivity, mechanical modulus and thermal conductivity along with a substantial reduction in loss tangent compared with neat PEI. In addition, the PEI/BNNSs nanocomposites exhibit better thermal stability with respect to neat polymers, which can withstand higher operating temperature (≥ 150 ºC) than both LDPE and PP. Remarkably, a greatly improved thermal conductivity of nearly 5-time higher than neat polymer is obtained in the PEI nanocomposite with 14 wt% BNNSs. These results suggest a promising route to high-performance insulation materials with desirable thermo-mechanical and thermo-dielectric strengths. The prepared composites are envisioned to allow the relief of temperature-gradient distribution and enable the improvement of heat dissipation in HVDC equipment. As the accumulation of space charge in insulation materials has a large effect on HVDC transmission systems, the study of charge injection and distribution of the resulting nanocomposites will be reported in due course.

ACKNOWLEDGEMENT

The authors would like to thank Dr. Feihua Liu, Mr. Xin Chen and Mr. Tian Zhang for fruitful discussions. H. Li acknowledges the financial support from the China Scholarship Council (CSC).

REFERENCES

[1] Q. Li *et al*, "Flexible high-temperature dielectric materials from polymer nanocomposites," Nature, vol. 523, no. 7562, pp. 576-579, 2015.

[2] H. Li *et al,* "Synergetic enhancement of mechanical and electrical strength in epoxy/silica nanocomposites via chemically-bonded interface," Compos. Sci. Technol., vol. 167, pp. 539-546, 2018.

[3] H. Li, F. Liu, B. Fan, D. Ai, Z. Peng and Q. Wang, "Nanostructured ferroelectric-polymer composites for capacitive energy storage," Small Methods, vol. 2, no. 6. pp. 1700399, 2018.

[4] Y. Zhou, S. Peng, J. Hu and J. He, "Polymeric insulation materials for HVDC cables: development, challenges and future perspective," IEEE Trans. Dielectr. Electr. Insul., vol. 24, no. 3, pp. 1308-1318, 2017.

[5] G. C. Montanari *et al*, "Next generation polymeric high voltage direct current cables—A quantum leap needed?," IEEE Electr. Insul. Mag., vol. 34, no. 2, pp. 24-31, 2018.

[6] H. Li *et al,* "Influences of semi-conductive coatings on the electric field distribution of GIS spacer interface," I*EEE Conf. Prop. Appl. Dielectr. Mater. (ICPADM),* 2015, pp. 887-890.

[7] T. L. Hanley, R. P. Burford, R. J. Fleming and K. W. Barber, "A general review of polymeric insulation for use in HVDC cables," IEEE Electr. Insul. Mag., vol. 1, no. 19, pp. 13-24, 2003.

[8] M. S. Khalil, "International research and development trends and problems of HVDC cables with polymeric insulation," IEEE Electr. Insul. Mag., vol. 6, no. 13, pp. 35-47, 1997.

[9] I. L. Hosier, A. S. Vaughan and S. G. Swingler, "An investigation of the potential of polypropylene and its blends for use in recyclable high voltage cable insulation systems," J. Mater. Sci., vol. 46, no. 11, pp. 4058-4070, 2011.

[10] Y. Zhou, J. He, J. Hu, X. Huang and P. Jiang, "Evaluation of polypropylene/polyolefin elastomer blends for potential recyclable HVDC cable insulation applications," IEEE Trans. Dielectr. Electr. Insul., vol. 22, no. 2, pp. 673-681, 2015.

[11] B. X. Du, H. Xu and J. Li, "Effects of mechanical stretching on space charge behaviors of PP/POE blend for HVDC cables," IEEE Trans. Dielectr. Electr. Insul., vol. 24, no. 3, pp. 1438-1445, 2017.

[12] X. Huang, Y. Yan, J. Zhang and P. Jiang, "Polypropylene based thermoplastic polymers for potential recyclable HVDC cable insulation applications," IEEE Trans. Dielectr. Electr. Insul., vol. 24, no. 3, pp. 1446-1456, 2017.

[13] N. Pfeiffenberger *et al*, "High temperature dielectric polyetherimide film development," IEEE Trans. Dielectr. Electr. Insul., vol. 25, no. 1, pp. 1446-1456, 2018.

[14] X. Huang, P. Jiang and T. Tanaka, "A review of dielectric polymer composites with high thermal conductivity," IEEE Electr. Insul. Mag., vol. 27, no. 4, pp. 8-16, 2011.

[15] D. Fabiani *et al,* "HVDC cable design and space charge accumulation. Part 3: Effect of temperature gradient," IEEE Electr. Insul. Mag., vol. 24, no. 2, pp. 5-14, 2008.

[16] Q. Li, F. Z. Yao, Y. Liu, G. Zhang, H. Wang and Q. Wang, "High-temperature dielectric materials for electrical energy storage," Annu. Rev. Mater. Res., vol. 48, pp. 219-243, 2018.

[17] S. Amin and M. Amin, "Thermoplastic elastomeric (TPE) materials and their use in outdoor electrical insulation," Rev. Adv. Mater. Sci., vol. 29, pp. 15-30, 2011.

[18] C. Zhi, Y. Bando, C. C. Tang, H. Kuwahara and D. Golberg, "Large-scale fabrication of boron nitride nanosheets and their utilization in polymeric composites with improved thermal and mechanical properties," Adv. Mater., vol. 21, no. 28, pp. 2889-2893, 2009.

[19] Q. Li *et al*, "Solution-processed ferroelectric terpolymer nanocomposites with high breakdown strength and energy density utilizing boron nitride nanosheets," Energy Environ. Sci., vol. 8, no. 3, pp. 922-931, 2015.

[20] R. Geick, C. H. Perry and G. Rupprecht, "Normal modes in hexagonal boron nitride," Phys. Rev., vol. 146, no. 2, pp. 543-547, 1966.

[21] F. Liu *et al*, "Poly(methyl methacrylate)/boron nitride nanocomposites with enhanced energy density as high temperature dielectrics," Compos. Sci. Technol., vol. 142, pp. 139-144, 2017.

[22] B. X. Du, X. X. Kong, B. Cui and J. Li, "Improved ampacity of buried HVDC cable with high thermal conductivity LDPE/BN insulation," IEEE Trans. Dielectr. Electr. Insul., vol. 24, no. 5, pp. 2667-2676, 2017.

[23] D. L. Zhang *et al*, "High thermal conductivity and excellent electrical insulation performance in double-percolated three-phase polymer nanocomposites," Compos. Sci. Technol., vol. 144, pp. 36-42, 2017.
[24] A. Azizi *et al*, "High-performance polymers sandwiched with chemical vapor deposited hexagonal boron nitrides as scalable high-temperature dielectric materials," Adv. Mater., vol. 29, no. 35, pp. 1701864, 2017.
[25] M. Ieda, "Dielectric breakdown process of polymers," IEEE Trans. Dielectr. Electr. Insul., vol. EI-15, no. 3, pp. 206-224, 1980.

He Li (S'16) was born in Zhejiang, China, in 1992. He received the B.Eng. degree in Electrical Engineering from Nanjing Agricultural University, China, in 2013. He is currently a Ph.D. student majoring in Electrical Engineering at Xi'an Jiaotong University and a jointly advised student in the Department of Materials Science and Engineering at the Pennsylvania State University, University Park, PA, USA. His research interests focus on dielectric polymers and polymer nanocomposites for energy storage and the studies of the interfacial effect in multicomponent high-voltage insulation systems.

Qisheng Ding was born in Jiangsu, China, in 1995. He is currently carrying out undergraduate research under Professor Qing Wang's supervision in the Department of Materials Science and Engineering at the Pennsylvania State University, University Park, PA, USA. His research interests focus on dielectric polymers and polymer nanocomposites for energy storage applications.

Lulu Ren was born in Shanxi, China, in 1994. She received the B.Eng. degree in Electrical Engineering from China University of Petroleum (East China), China, in 2015. She is currently a jointly advised Ph.D. student in the Department of Materials Science and Engineering at the Pennsylvania State University, University Park, PA, USA. Her research interests focus on dielectric ceramics and polymer nanocomposites for energy storage applications.

Ding Ai was born in Hubei, China, in 1993. She received the B.Eng. degree in Materials Science and Engineering from China University of Geosciences, Wuhan, China, in 2014. She is currently a jointly advised Ph.D. student in the Department of Materials Science and Engineering at the Pennsylvania State University, University Park, PA, USA. Her research interests focus on dielectric ceramics and polymer-based composites for energy storage applications.

Zongliang Xie was born in Jiangsu, China, in 1996. He received the B.Eng. degree in Electrical Engineering from Xi'an Jiaotong University, China, in 2018. He is currently a graduate student majoring in Electrical Engineering at Xi'an Jiaotong University. His research interests focus on the study of the mechanisms and measurement technologies of space charge in dielectrics and polymer composites.

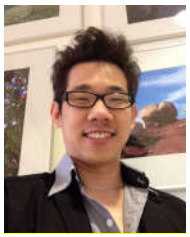

Wuttichai Reainthippayasakul was born in Bangkok, Thailand. He received the B.Sc. degree in Chemistry from Chulalongkorn University, Thailand, in 2006, and M.Sc. degree in Materials Science and Engineering from the Pennsylvania State University, University Park, PA, USA, in 2014. He is currently a Ph.D. student at the Pennsylvania State University, University Park, USA. His research interests focus on polymer nanocomposites for dielectrics and electronic devices.

Yuqi Huang was born in Sichuan, China, in 1995. She carried out undergraduate research under Professor Qing Wang's supervision at the Department of Materials Science and Engineering at the Pennsylvania State University, University Park, PA, USA. Her research interests focused on dielectric polymers and polymer nanocomposites for energy storage applications.

Lilan Liu was born in Jiangsu, China, in 1991. She received the B.Eng. degree in Electrical Engineering from Xi'an Jiaotong University, China, in 2014. She is currently a Ph.D. student majoring in Electrical Engineering at Xi'an Jiaotong University. Her research interests focus on the calculation and optimization of insulation structures for high-voltage power equipment, the dielectric and mechanical properties of insulation materials.

Zongren Peng was born in Shaanxi, China. He graduated from Xi'an Jiaotong University, China, in 1977, majoring in Electrical Engineering. He is a Professor of Electrical Engineering at Xi'an Jiaotong University. His research interests lie in the calculation and optimization of insulation structures for ultra-high voltage power equipment, the mechanisms and measurement technologies of space charge in dielectrics, polymeric materials for electrical insulation applications, and the studies of the interfacial effect in multicomponent high-voltage insulation systems. He is a Distinguished Expert in SGCC (State Grid Corporation of China).

Qing Wang was born in Hubei, China. He received the Ph.D. degree in Chemistry from the University of Chicago, in 2000. He is a Professor of Materials Science and Engineering at the Pennsylvania State University, University Park, PA, USA. His research interests are centered on the development of functional materials including ferroelectric polymers, electroactive polymers and polymer–ceramic nanocomposites for applications in electronics and energy storage and energy harvesting.